THE JOURNAL OF
PHYSICAL
CHEMISTRY A

VOLUME 105, NUMBER 45, NOVEMBER 15, 2001

ARTICLES

New Insight into the Excited-State Proton-Transfer Reactions of 1-Naphthylamine in Solution

Ali A. El-Rayyes,[†,‡] H. P. Perzanowski,[†] Sami A. I. Barri,[†] and Uwe K. A. Klein*[,†,‡]

Chemistry Department, King Fahd University of Petroleum and Minerals, Dhahran 31261 Saudi Arabia, and Laser Research Section, King Fahd University of Petroleum and Minerals, Dhahran 31261 Saudi Arabia

Received: April 10, 2001; In Final Form: September 4, 2001

Proton-transfer reactions from the excited state of 1-naphthylamine (RNH_2) have been investigated in aqueous solutions of various $HClO_4$ concentrations. The system is found to contain three species rather than simply the acidic and the neutral form of RNH_2 as previously believed. The new species X, can be clearly detected at $[HClO_4] \geq 5$ M, in both absorption and emission. X is proposed to be an adduct of RNH_2 and an unhydrated $HClO_4$, i.e., $X \equiv RNH_2\text{- - -}H^+\text{- - -}ClO_4^-$. Absorption and fluorescence spectra of X are shown. Quantum yields of the three excited species RNH_2*, RNH_3^+*, and X* have been found to be 0.49, 0.327, and 0.065, respectively. A kinetic scheme is presented indicating that the proton transfer from RNH_3^+* depends on the availability of free water, i.e., water that can accept protons. All rate constants have been determined. A theoretical model for the hydration of protons shows that as long as there is excess free water an average of 9 water molecules are used for the hydration of one proton.

1. Introduction

Proton dissociation and association in the excited state of aromatic compounds are elementary processes in photochemistry and in biochemistry. The acid−base properties of aromatic compounds in their excited state are closely related to the corresponding electronic structure. Since the pioneering work of Förster[1] and Weller,[2] a number of studies on the acidity constant pK_a* in the excited state by means of nanosecond spectroscopy with fluorimetry have been reported. Intermolecular proton transfer between the excited molecules and the solvent has been investigated in the past few years by means of picosecond spectroscopic techniques. Such studies[3−11] are essential to gain more insight into the important role of the proton acceptor, usually the solvent, in condensed phase proton-transfer reactions. No proton can be transferred without a proper acceptor, and its dynamics depends on the number of solvent molecules that can accept the detached proton. Water is generally regarded as an ideal proton acceptor and its dynamics in the proton-transfer kinetics has been studied substantially in alcohol−water mixtures. A water cluster containing 4 ± 1 water molecules has been proposed to be the proton acceptor in the case of photoexcited 2-naphthol in methanol−water mixtures.[3] Huppert et al.[7] have also suggested an involvement of a single water molecule in the early stage of the proton-transfer reaction. Htun et al.[6] have studied the proton-transfer reactions of 4-hydroxy-1-naphthalenesulfonate in alcohol−water mixtures and proposed the participation of a water dimer or a cluster of two water molecules in the hydration of the proton. Another independent study on the quenching of the fluorescence emission of 5-cyano-2-naphthol and 5,8-dicyano-2-naphthol has also shown a water dimer to be the effective proton acceptor.[8]

In the gas-phase proton-transfer reactions the acid−base dimer exists as a hydrogen-bonded adduct; however, it can be converted to an ion pair in the presence of water molecules that

---

* Author to whom correspondence should be addressed. E-mail: ukaklein@kfupm.edu.sa.

[†] Chemistry Department.

[‡] Laser Research Section.

10.1021/jp011340p CCC: $20.00

promote the proton transfer leading to the formation of an ion pair complex.[12]

The fluorescence emission and proton quenching of the fluorescence of naphthylamines has been investigated by many authors.[13−21] In all the studies, it was found that the decay of the excited state of neutral amine $(RNH_2)^*$ is appreciably fast in comparison with the rate of proton association reaction. This leads to a weak coupling reaction in the excited state which results in a weak fluorescence emission from the protonated amine (RNH_3^{+*}).

Förster,[14,15] and also Schulman and Liedke[16] have shown that the fluorescence of naphthylamines is initially quenched by protons but reappears at high acid concentrations. For the quenching mechanism, Förster suggested an intermediate in which a proton is shared between β-naphthylamine and one water molecule. Schulman and Liedke proposed an intermediate complex formed between the naphthylammonium ion and one water molecule. Tsutsumi and Shizuka[17−21] attributed the quenching to an interaction between the π-system of the excited naphthylamine ring $(RNH_2)^*$ and H^+, other than protonation of the nitrogen atom of $(RNH_2)^*$. This is in accordance with Weller's prediction,[13] that the neutral naphthylamine in the excited-state becomes susceptible toward electrophilic protonation at one of the aromatic carbon atoms.

Although the kinetic treatment of the neutral form (RNH_2^*) has been accomplished, this is not the case for the acidic form (RNH_3^{+*}) where quantum yields have been measured but are not quantitatively interpreted. Furthermore, it was reported[17] that the fluorescence decay time of the excited acid was nonexponential and is increasing with the acidity of the medium (47 ns at 13 M H_2SO_4). However, in our investigations we found it to be biexponential with a long-living component that agrees well with the reported ones for the $(RNH_3^+)^*$ and a fast decay component which was not reported before. In this paper, a detailed kinetic study of the acidic form of the excited 1-naphthylamine is presented along with a report on a newly discovered fluorescent species of 1-naphthylamine present at high acid concentrations. The acid used in this study is $HClO_4$ as it is known to provide long-term stability of highly acidic solutions.

2. Experimental Section

Materials. 1-Naphthylamine was provided by Fluka company and was used after recrystallization from petroleum ether followed by sublimation. $HClO_4$ (>70%) Fluka was used. Throughout the experiments, deionized water was used for sample preparations.

Sample Preparations. A diluted solution of the acid was used to prepare samples of pH 0.2 to pH 2.0. For pH values from 3.0 to 9.0, buffer (pH 3, 6, and 9) solutions were used; highly acidic solutions of 1-naphthylamine were prepared by adding different volumes of concentrated perchloric acid to the same volume of the amine−water solution. The naphthylamine concentration was kept at $C_0 = 4.92 \times 10^{-5}$ M.

UV−Vis Absorption Measurements of the Solutions Used. Steady-state UV−Vis absorption measurements for solutions were obtained using a λ-5 (Perkin-Elmer) Spectrophotometer.

Fluorescence Emission Measurements. Fluorescence spectra were recorded with a SPF-500 spectrofluorometer from SLM Instruments. The fluorescence spectra were corrected for the intensity of the lamp and the sensitivity of the photomultiplier tube.

Fluorescence Decay Time Measurements. A mode-locked Nd:YAG laser (Spectra-Physics model 3800) with a mode locker (Spectra-Physics model 451) operating at 82 MHz repetition rate was used to pump a rhodamine 6G dye laser. Cavity dumping at 4 MHz was performed. The output pulses were frequency doubled (Spectra-Physics model 390 frequency doubler). The excitation wavelength was 300 nm and the fluorescence decay signals of the probe molecule were collected at the wavelength of maximum fluorescence emission. Lifetimes were measured using the Applied Photophysics photon-counting spectrometer system, model PS 60, equipped with a XP 2020Q photomultiplier. The actual pulse width of the excitation pulse is less than 10 ps; however, due to the response time of the photon counting system it is broadened to 350 ps. Data were collected through a multichannel analyzer and then transferred to a computer for analysis.

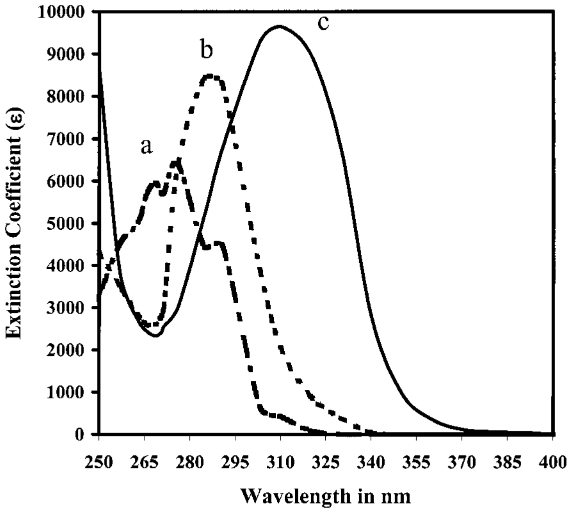

Figure 1. Absorption spectra of (a) RNH_3^+, (b) X, and (c) RNH_2.

3. Results

3.1. Absorption Spectra. Absorption spectra of solutions of high pH values show a broad structureless band specific to the absorption of the neutral form of 1-naphthylamine, Figure 1c. However, starting from solutions with pH 2.0, addition of more acid leads to a blue shift with the appearance of a structured absorption band corresponding to the absorption of the protonated form RNH_3^+, Figure 1a. By increasing the acidities of the solutions we found a red shift in the absorption spectra with an isosbestic point at 276 nm as shown in Figure 2. These results indicate the presence of a species in the ground state other than both the neutral and the protonated forms of 1-naphthylamine, Figure 1b.

3.2. Emission Spectra. Emission spectra of the neutral form RNH_2 showed a strong quenching effect upon increasing the hydrogen ion concentration from $[H^+] \geq 0.01$ to $[H^+] < 0.80$ M) without increasing the fluorescence intensity of the protonated form. This is in accordance with the reported findings.[14,17] However, at $[H^+] \geq 0.80$ M, where there is no RNH_2 and excitation is at 276 nm, an increase in the fluorescence intensity of RNH_3^{+*} was observed (Figure 3a) with a slight broadening at high acid molarity. In earlier measurements,[14,17] this was interpreted as a probable slight broadening of the fluorescence of the acidic form due to an increase of the acid concentration. However, a close look at the absorption spectra suggests that the emission was not only from RNH_3^{+*} but also from another species present in the solution. The fluorescence spectra for RNH_2^*, RNH_3^{+*}, and that for the new species are shown in Figure 4. Absorption and fluorescence emission spectra of the

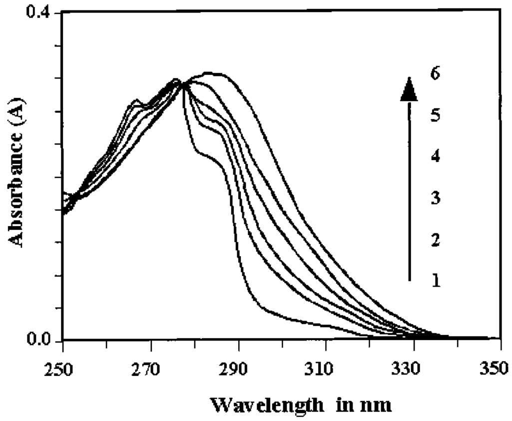

Figure 2. Absorption spectra of RNH_3^+ at different acidic concentrations, (1) 0.80 M $HClO_4$, (2) 5.88 M, (3) 6.34 M, (4) 7.81 M, (5) 9.76 M, (6) 11.2 M.

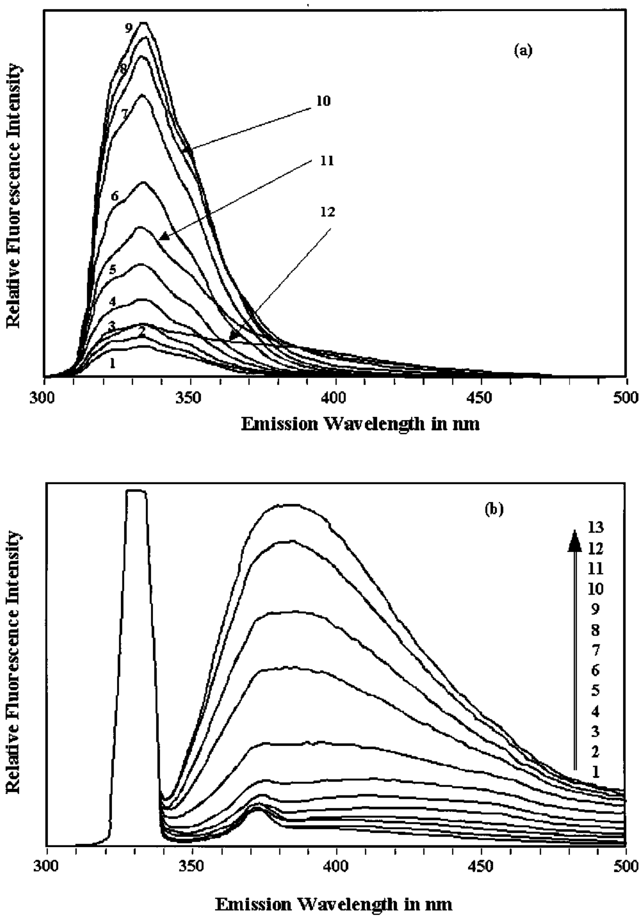

Figure 3. Fluorescence emission spectra of (a) RNH_3^{+*} in different acidic solutions, λ_{exc} 276 nm, (1) 0.80 M $HClO_4$, (2) 1.60 M, (3) 2.44 M, (4) 3.22 M, (5) 4.00 M, (6) 4.88 M, (7) 5.88 M, (8) 6.34 M, (9) 7.32 M, (10) 7.81 M, (11) 9.76 M, (12) 11.2 M. (b) X* in different acidic solutions, λ_{exc} 330 nm, (1) 0.80 M $HClO_4$, (2) 1.60 M, (3) 2.44 M, (4) 3.22 M, (5) 4.00 M, (6) 4.88 M, (7) 5.88 M, (8) 6.34 M, (9) 7.32 M, (10) 7.81 M, (11) 8.87 M, (12) 9.76 M, (13) 11.2 M.

new species (X) are shown in Figure 5. It can be seen that the absorption and fluorescence emission spectra of X are nearly mirror images of each other.

3.3. Fluorescence Decay Measurements. Fluorescence decays of RNH_2* in aqueous solutions of various pH values (pH 0.2 to 9.0) recorded at λ_{em} = 470 nm show that the decays are biexponential and nicely fit the equation

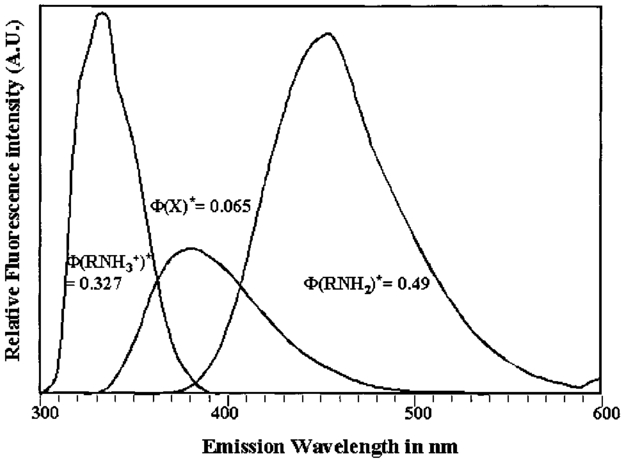

Figure 4. Fluorescence emission of RNH_3^{+}*, X*, and RNH_2*.

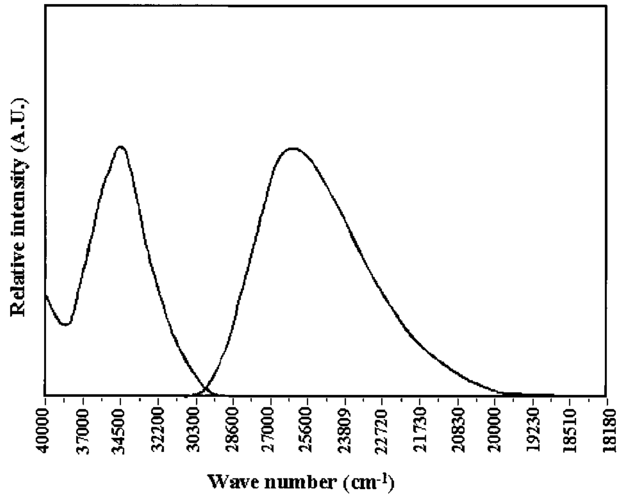

Figure 5. Absorption and fluorescence spectra of X.

TABLE 1: Fluorescence Decay Time Constants[a] for RNH_2*

pH	τ_1	A_1	τ_2	A_2
0.20	1.13	0.813	2.23	1.37
0.50	1.88	1.15	1.88	1.10
0.70	0.551	−0.675	2.01	3.92
1.0	0.662	−0.333	2.19	1.40
1.20	1.48	−6.59	2.09	8.53
1.40	1.77	−7.23	2.91	9.24
1.70	2.14	−5.38	4.01	4.11
1.90	2.22	−1.35	6.43	3.63
2.0	2.14	−0.777	7.64	2.62
3.0	2.07	−0.313	15.6	2.51
6.0	18.13	2.11		
9.0	18.24	2.12		

[a] λ_{exc} = 300 nm, λ_{em} = 470 nm.

$$I(t) = A_1 e^{t/\tau_1} + A_2 e^{t/\tau_2} \quad (1)$$

A free 4-parameters fit for various pH values is shown in Table 1. In general, both time constants decrease with decreasing pH in agreement with the results reported by Shizuka et al.,[17] i.e., an equilibrium between excited acidic and neutral forms with quenching of the neutral form by H^+. A further increase in the acid concentration 0.08 M ≤ $[H^+]$ ≤ 4 M, where only the acidic form exists in the excited state, the decays are single exponential with an increase in the lifetimes as the acidity increases. This

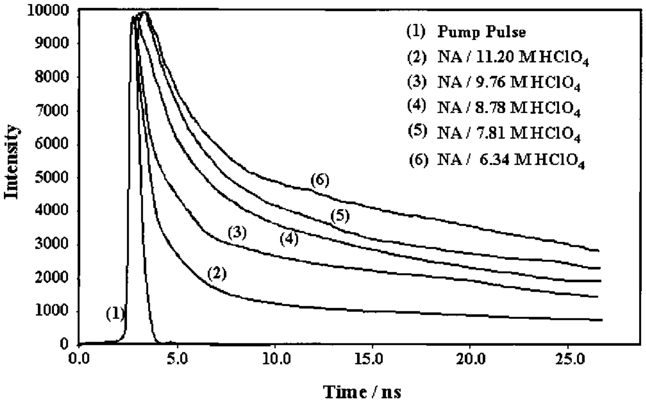

Figure 6. Emission decay profile of 1-naphthylamine in highly acidic aqueous solutions.

TABLE 2: Fluorescence Decay Time Constants^a for $RNH_3^{+}*$

$[H^+]$	τ_1	A_1	τ_2	A_2
0.1	1.75	4.13		
0.80	1.98	2.35		
1.60	2.88	4.62		
2.44	3.79	4.21		
3.22	5.58	4.52		
4.00	8.14	2.31		
4.88	1.49	1.05	14.50	1.68
5.88	1.59	1.44	16.20	1.44
6.34	1.72	1.48	28.55	1.34
7.32	1.75	1.22	38.55	1.48
7.81	1.85	1.45	41.44	1.68
8.78	1.88	1.14	44.99	1.64
9.76	1.94	1.08	38.42	0.540
11.2	1.98	1.22	31.05	0.285

^{a} $\lambda_{exc} = 300$ nm, $\lambda_{em} = 334$ nm.

observation suggests that dissociation of the proton from excited $RNH_3^{+}*$ occurs exclusively with no recombination reaction in the excited state. These measurements are in agreement with the reported results.[17] However, in solutions with high acid concentrations, $[H^+] \geq 4.88$ M, the decays ($\lambda_{em} = 330$ nm), Figure 6, need to be fitted to a biexponential function (Table 2) with a long living component and a fast decaying one. The long living component can be assigned to the $RNH_3^{+}*$, and the short living component is assigned to a new emitting species X*. Recording the emission decays at $\lambda_{em} = 380$ nm shows almost only the fast decay, i.e., the decay of X*. This confirms what we have seen in the fluorescence emission results. Observation of X was not seen or reported before.

4. Discussion

The experimental results suggest the formation of a new species in the ground state of 1-naphthylamine at high acid concentration, which needs to be taken into account for a quantitative kinetic study. A kinetic model representing the proton-transfer reaction of 1-naphthylamine is given in Scheme 1. In the scheme, ϵ and $(1 - \epsilon)$ are the absorption fractions and k_f and k_{fx} are the fluorescence rate constants for $RNH_3^{+}*$ and X*, respectively, k_d and k_{dx} are the deactivation rate constants, k_1 is a quasi first-order rate constant, and $k^{\backslash}_f$ and $k_d^{\backslash}$ are the fluorescence and quenching rate constants for RNH_2*.

The pK_a value of 1-RNH_2 is 3.9, and therefore in the presence of protons (1×10^{-2} M), 1-RNH_2 is completely protonated at the nitrogen atom in the ground state. The absorption spectrum is similar to that of naphthalene. However, upon excitation, fluorescence comes from the excited RNH_2 and is very strong since the proton dissociation rate constant in the excited state of 1-RNH_3^+ is very fast ($\approx 10^9$ s^{-1}). As a result, the fluorescence emission intensity of 1-$RNH_3^{+}*$ is very weak. The fluorescence quantum yield of RNH_2* was reported[13] to be 0.49. On increasing the hydrogen ion concentration, the emission comes only from $RNH_3^{+}*$ and is characterized by a structured band with a maximum at 334 nm. Table 2 summarizes the lifetimes and the preexponential factors of RNH_3^+ in the excited state. It is obvious that the lifetime of the long living component increases with the acid concentration until it reaches a maximum at $[H^+] \geq 7.32$ M and then it decreases. At very high acid concentrations, $[H^+] \geq 4.88$ M, a new emission band starts to appear, accompanied by a decrease in the fluorescence intensity of the 334 nm band. This new emission band plays an important role in decreasing the lifetimes and the quantum yields of $RNH_3^{+}*$ (see Figure 3a). It is known that free water molecules are needed as a proton acceptor for the proton to be transferred. The excited-state acid–base reaction of RNH_3^+ is highly influenced by the presence of free water molecules in solution. The idea of free water already existed in the late 1970s.[22]

SCHEME 1: Proton-Transfer Reaction of 1-Naphthylamine in Acidic Medium

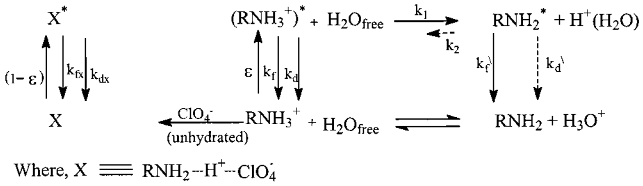

4.1. Quantum Yields and Lifetime Analysis. *a. Analysis of RNH_2**. From the steady-state approximation, Shizuka et al. obtained the following equation:[17]

$$\frac{\Phi_{max}}{\Phi} = 1 + \frac{k_d^{\backslash}}{k_f'}[H^+(H_2O)] \tag{2}$$

A plot of our values Φ_{max}/Φ vs $[H^+]$ yields a linear Stern–Volmer relationship. Using a value of 4.8×10^7 s^{-1} for $k^{\backslash}_f$ from lifetime measurements, $k_d^{\backslash}$ is determined to be 8.6×10^9 M^{-1} s^{-1} which is in very good agreement with the value of 8.9×10^9 M^{-1} s^{-1} reported in the literature.[14,17]

*b. Analysis of RNH_3^{+}**. If coupling between the excited states of $RNH_3^{+}*$, RNH_2*, and/or X* is negligible at high $HClO_4$, the following equation can be obtained:

$$\frac{\Phi_{max}}{\Phi} = 1 + \frac{k_1}{k_f + k_d}[H_2O]_{free} \tag{3}$$

To calculate the relative quantum yields, we have to determine ϵ, the fraction of the absorbance due to RNH_3^+, at the various concentrations of $[H^+]$. Separation of the absorption spectra into the components RNH_3^+ and X yield the absorption fractions ϵ and $1 - \epsilon$ presented in Table 3, where $1 - \epsilon = [X]/C_0$, C_0 is the initial concentration of the 1-naphthylamine solution. The quantum yields of $RNH_3^{+}*$ have to be corrected for the absorption fraction ϵ. This leads to a quantum yield value of $\Phi_{max} = 0.327$, which is larger than the literature value[17] of 0.25. From the limiting value for $(\Phi_{max.}/\Phi)$ as the hydrogen ion concentration goes to zero, and knowing that τ^0_{AH} is 44.99 ns, then k_f and k_d are found to be 7.3×10^6 s^{-1}and 1.5×10^7 s^{-1}, respectively. Inserting these values in eq 3, using $[H_2O]_{free}$ to be 55.5 M, $k_1^{\backslash}$ which is equal to $k_1[55.5]$ is calculated to be 3.8×10^8 s^{-1}. The values of these rate constants allow us to calculate the mole fractions of free water $\gamma[H_2O]_{free}$ in solutions

TABLE 3: Absorption Fractions of X and RNH_3^+

[$HClO_4$]	[X]/M	$1 - \epsilon \equiv [X]/C_0$ [a]	$\epsilon \equiv \{C_0 - [X]\}/C_0$
0.80	1.72×10^{-6}	0.035	0.965
1.60	1.72×10^{-6}	0.035	0.965
2.44	2.52×10^{-6}	0.051	0.949
3.22	2.65×10^{-6}	0.054	0.946
4.00	2.65×10^{-6}	0.054	0.946
4.88	3.44×10^{-6}	0.070	0.930
5.88	4.47×10^{-6}	0.091	0.909
6.34	6.00×10^{-6}	0.122	0.878
7.32	9.05×10^{-6}	0.184	0.816
7.81	1.49×10^{-5}	0.304	0.696
8.78	1.97×10^{-5}	0.401	0.599
9.76	2.48×10^{-5}	0.505	0.495
11.2	2.70×10^{-5}	0.550	0.450

[a] $C_0 = 4.92 \times 10^{-5}$ M.

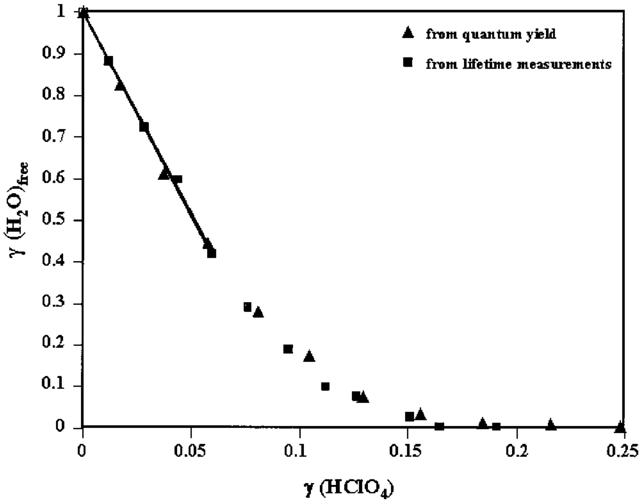

Figure 7. A plot of the mole fractions of free water vs the mole fractions of the perchloric acid, ▲ indicates values calculated from quantum yield measurements, ■ indicates values calculated from lifetime measurements.

of different acidity according to eq 3a:

$$\gamma(H_2O)_{free} = \left(\frac{\Phi_{max}}{\Phi} - 1\right)\frac{k_f + k_d}{k_1} \tag{3a}$$

Values of $\gamma(H_2O)_{free}$ determined from quantum yield measurements (eq 3a) and from fluorescence lifetime measurements (long component) using the following equation:

$$\gamma(H_2O)_{free} = \left(\frac{\tau_{max}}{\tau} - 1\right)\frac{k_f + k_d}{k_1} \tag{4}$$

are presented in Figure 7. The slope of the figure at the linear part is around −9.76, which means that, as long as a lot of free water is available, one proton on average binds 9 water molecules as a cluster or hydration shell. At low acid concentration, $[H^+] \geq 4.0$ M, there are a lot of free water molecules to be used. This is shown in the linear part of the plot. However, by increasing the acidity, a point is reached ($\gamma[HClO_4] \geq 0.07$) at which there are not enough free water molecules to make up the same hydration shell. In this case the hydration sphere shrinks leading to the curvature in the plot. At $\gamma(HClO_4)$ equal to 0.20, no more free water is available, corresponding to a hydration shell of 4 water molecules per proton. At this point there is no more proton-transfer reaction and both the quantum yield and lifetime of RNH_3^{+*} reach the maximum. Then further acid added does not dissociate anymore. A competition between the $ClO_4^-{}_{(unhydrated)}$ and the protons exist to the extent that the ClO_4^- may remain unhydrated. RNH_3^+ may share a proton with $ClO_4^-{}_{(unhydrated)}$ to form the new emitting species X. This is equivalent to an adduct formation like $[RNH_2\text{- - -}HClO_4 \equiv RNH_2\text{- - -}H^+\text{- - -}ClO_4^-]$. We may reiterate from these results that high acidity does not only mean large number of protons but also less and less free water.

SCHEME 2: Hydration of Protons

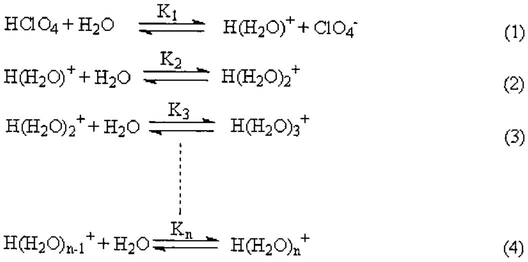

$$HClO_4 + H_2O \underset{}{\overset{K_1}{\rightleftharpoons}} H(H_2O)^+ + ClO_4^- \tag{1}$$

$$H(H_2O)^+ + H_2O \overset{K_2}{\rightleftharpoons} H(H_2O)_2^+ \tag{2}$$

$$H(H_2O)_2^+ + H_2O \overset{K_3}{\rightleftharpoons} H(H_2O)_3^+ \tag{3}$$

$$H(H_2O)_{n-1}^+ + H_2O \overset{K_n}{\rightleftharpoons} H(H_2O)_n^+ \tag{4}$$

c. Kinetic Model for the Hydration of Protons. The hydration of protons may be viewed in terms of the following treatment. Hydration of perchloric acid in water follows the equations in Scheme 2. In Scheme 2, n_o is the initial number of moles of $HClO_4$, and n_{H_2O} is the initial number of moles of water in solution, with $n_{H_2O} > n_o$. Then for eq 1, in Scheme 2, at equilibrium we have $n_o(1 - \alpha_1)$ moles of $HClO_4$, $(n_{H_2O} - \alpha_1 n_o)$ moles of water, $\alpha_1 n_o$ moles of $H(H_2O)^+$, and $\alpha_1 n_o$ moles of perchlorate anions, where α_1 is the degree of hydration with one H_2O molecule. For the equations in Scheme 2, α_i is the degree of hydration with i H_2O molecules

Applying the same principle to the general eq 4, Scheme 2, leads to, $n_o[\alpha_1\alpha_2\alpha_3\alpha_{n-1}(1 - \alpha_{n-1})]$ moles of $HClO_4$, $[n_{H_2O} - n_o(\alpha_1 + \alpha_1\alpha_2 + \alpha_1\alpha_2\alpha_3\ \alpha_1\alpha_2\alpha_3\alpha_{n-1}(1 + \alpha_n))]$ moles of H_2O, and $n_o[\alpha_1\alpha_2\alpha_3\ ...\ \alpha_n]$ moles of $H(H_2O)_n^+$, where n is the maximum hydration number. The number of moles of $H(H_2O)_i^+$, n_i, is given by eq 5, with $i = 1$ to $n - 1$:

$$n_i = n_0(1 + \alpha_{i+1})\prod_{j=1}^{i}\alpha_j \tag{5}$$

$$n_{H_2O}(\text{free}) = n_{H_2O} - n_o(\alpha_1 + \alpha_1\alpha_2 + \alpha_1\alpha_2\alpha_3 + ... + \alpha_1\alpha_2\alpha_3 ... \alpha_{n-1}(1 + \alpha_n)) \tag{6}$$

which can be written as

$$n_{H_2O}(\text{free}) = n_{H_2O} - n_o[\sum_{i=1}^{n-2}\beta_i + \beta_{n-1}(1 + \alpha_n)]$$

$$\text{with, } \beta_i = \prod_{j=1}^{i}\alpha_j \tag{7}$$

and further rearranged to the form

$$n_{H_2O}(\text{free}) = n_{H_2O} - n_o\sum_{i=1}^{n}\beta_i \tag{8}$$

Dividing the above equation by the total number of moles of $HClO_4$ and H_2O, and taking into account that $\gamma(HClO_4) + \gamma(H_2O) = 1$, leads to

$$\gamma_{H_2O}(\text{free}) = 1 - \gamma_{HClO_4}[1 + \sum_{i=1}^{n}\beta_i] \tag{9}$$

where γ's indicate the mole fractions.

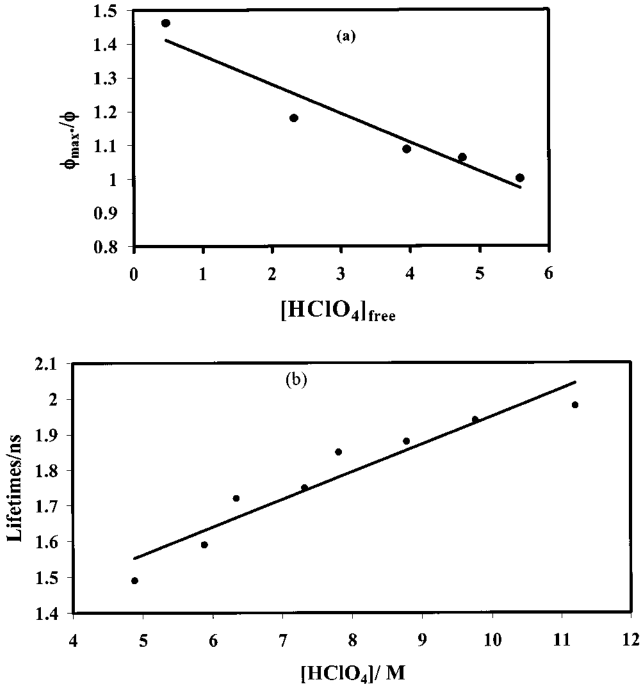

Figure 8. (a) Stern−Volmer plot of Φ_{max}/Φ for X vs the free perchloric acid concentration. (b) Fluorescence lifetimes of X vs the perchloric acid concentrations.

The limiting slope for $\gamma(HClO_4) < 0.07$ is equal to −9.76, and with eq 9, one obtains: $\sum_{i=1}^{n} \beta_i = 8.76$. It is, of course, known that α_i is a function of the [$HClO_4$] and the [H_2O].

*d. Analysis of X**. The fluorescence spectra of X are recorded after exciting the samples at $\lambda_{exc} = 330$ nm, where only X absorbs and fluoresces at a wavelength with maximum at 380 nm (Figure 3b). It is worth mentioning here that the slight peak at 370 nm is a Raman scattering peak. The relative quantum yields of X are calculated and corrected for the absorption fractions $(1 - \epsilon)$. A Stern−Volmer plot of the relative quantum yield of X vs the free perchloric acid shows that the quantum yield of X increases as the number of moles of free (unhydrated) perchloric acid increases, Figure 8a. From Table 3, the ratio of the number of moles of undissociated perchloric acid to the total number of moles is equal to 0.55. Referring to Scheme 2, $n(HClO_4) = 0.55n_o$, then

$$n(HClO_4) = \Phi/\Phi_{max} \times 0.55n_o$$
$$= (1 - \alpha_1)n_o \qquad (10)$$

Equation 10 is used to calculate α_1 at different acid concentration. The result is plotted in Figure 9. From the figure it is obvious that the first few points are almost the same, i.e., $\alpha_1 \approx 1$ at high free water concentration. The result suggests that we may consider the fluorescence intensity of X to be directly proportional to the concentration of unhydrated ClO_4^-, that is the structure of X is likely be an adduct formation such as $[RNH_2\text{- - -}H^+\text{- - -}ClO_4^- \equiv RNH_2\text{- - -}HClO_4]$. This is also supported by the fact that λ_{max} of both the absorption and emission spectrum of X are between the neutral (RNH_2) and the acidic form (RNH_3^+). In the acidic form the proton is localized at the nitrogen of the amino group. In X the proton is probably delocalized, i.e., shared between the RNH_2 and the ClO_4^-, having a lesser effect on the π-electron system (responsible for the transition in the UV region) than an H^+ localized at the amino group.

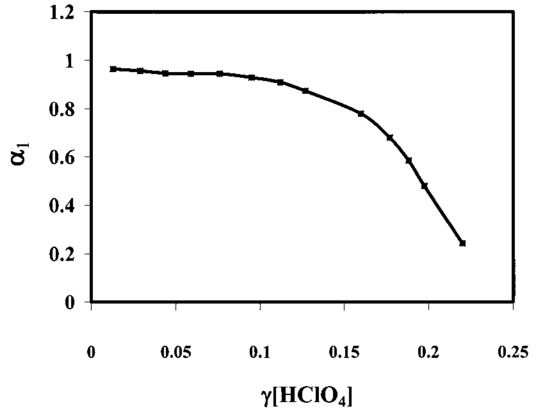

Figure 9. A plot of α_1, the degree of hydration with one water molecule, i.e., the degree of dissociation of $HClO_4$ vs the mole fractions of $HClO_4$.

TABLE 4: Fluorescence Quantum Yield, Lifetime, and Fluorescence Rate and Deactivation Rate Constants for the Three Species

	RNH_2*	RNH_3^{+}*	X*
Φ	0.49	0.327	0.065
τ /ns	18.24	44.99	1.98
k_f /s^{-1}	4.8×10^7	7.3×10^6	3.3×10^7
k_d/s^{-1}	8.6×10^9 [a]	1.5×10^7	4.7×10^8

[a] The unit is M^{-1} s^{-1}.

At high acid concentration, the decay of the RNH_3^{+}* became biexponential; the short living component (Table 2) is assigned to the fluorescence decay of X*. The maximum fluorescence quantum yield and lifetime of X* are 0.065 and 1.98 ns, respectively, then k_{fx} is 3.3×10^7 s^{-1}, which is about 4 times higher than the value of k_f of the protonated form and in reasonable agreement with the oscillator strength estimated from the absorption spectra.

Using the relation

$$\frac{1}{\tau_{max}} = k_{fx} + k_{dx} \qquad (11)$$

k_{dx} is found to be 4.7×10^8 s^{-1}. All the quantum yields and the fluorescence decay and quenching rate constants k_f and k_d for the three species are presented in Table 4. Figure 8b shows that the fluorescence lifetime of X increases linearly with the acidity of the medium. This suggests a linear decrease of free water traces which quench the fluorescence of X*. Consequently, fluorescence behavior of X may be used to trace the presence of water molecules and/or to study highly acidic “water-free” environments.

Conclusions

The proton-transfer reaction kinetics of 1-naphthylamine were studied by means of picosecond spectroscopy. We found that it is not a simple two-component system. The results found for the neutral form RNH_2* agree well with the literature values. Studies of the protonated form (RNH_3^{+}*) in highly acidic solutions of $HClO_4$ show the presence of another emitting species in the solution which was not reported before. The quantum yield of the RNH_3^{+}* is found to be 0.327 which is higher than the literature value where the new emitting species was not taken into considerations. The new emitting species, X $\equiv RNH_2\text{- - -}HClO_4$, is most likely formed in the absence of free water molecules. A kinetic model for the hydration of protons is proposed. According to the model, an average of 9 water molecules are found to be the proton acceptor when there are enough water molecules to be used. Increasing the number of moles of the acid decreases the number of water molecules in the hydration shell. In the absence of free water molecules the perchlorate anion shares a proton with the acidic form of the amine (RNH_3^{+*}) leading to the formation of X. The structure of X is proposed to be an adduct like [RNH_2- - -H^+- - -ClO_4^- ≡ RNH_2- - -$HClO_4$]. The quantum yield of X is found to be 0.065. All the fluorescence decay and quenching rate constants k_f and k_d have been determined. The excited-state acid−base reaction of 1-naphthylamine is very sensitive to the presence or absence of water molecules and/or protons. This makes it a good candidate to probe the acidity at interfaces and at catalyst surfaces.

Acknowledgment. Support from King Fahd University of Petroleum and Minerals is gratefully acknowledged. The authors also appreciate the support given by Dr. M. A. Garwan and Dr. H. Al-Masoudi from the Center for Applied Physical Sciences (CAPS), Research Institute. Helpful discussions with Professors A. Suwaiyan and F. Al-Adel are also gratefully acknowledged.

References and Notes

(1) Forster, Th. *Z. Electrochem*. **1950**, *54*, 42.
(2) Weller, A. *Z. Electrochem*. **1952**, *56*, 662; **1956**, *60*, 1144.
(3) Lee, J.; Griffin, R. D.; Robinson, G. W. *J. Chem. Phys*. **1975**, *82*, 4920.
(4) Suwaiyan, A.; Al-Adel, F.; Hamdan, A.; Klein, Uwe K. A. *J. Phys. Chem*. **1990**, *94*, 7423.
(5) Tolbert, L. M.; Harvey, L. C.; Lum, R. C. *J. Phys. Chem*. **1993**, *97*, 13335.
(6) Htun, M. T.; Suwaiyan, A.; Klein, Uwe K. A. *Chem. Phys. Lett*. **1995**, *243*, 71.
(7) Huppert, D.; Kolodney, E.; Gutman, M.; Nachliel, E. *J. Am. Chem. Soc*. **1982**, *104*, 6949.
(8) Tolbert, L. M.; Haubich, J. E. *J. Am. Chem. Soc*. **1994**, *116*, 10593.
(9) Htun, M. T.; Suwaiyan, A.; Klein, Uwe K. A. *Chem. Phys. Lett*. **1995**, *243*, 506.
(10) Htun, M. T.; Suwaiyan, A.; Klein, Uwe K. A. *Chem. Phys. Lett*. **1995**, *243*, 512.
(11) Htun, M. T.; Suwaiyan, A.; Klein, Uwe K. A. *Chem. Phys. Lett*. **1995**, *264*, 285.
(12) Snyder, J. A.; Cazar, R. A.; Jamka, A. J.; Tao, F. *J. Phys. Chem*. **1999**, *103*, 7719.
(13) Weller, A. *Prog. React. Kinet*. **1961**, *1*, 189.
(14) Forster, Th. *Pure Appl. Chem*. **1970**, *24*, 443.
(15) Forster, Th. *Chem. Phys. Lett*. **1972**, *17*, 309.
(16) Schulman, S. G.; Liedke, P. *Z. Physik. Chem. NF* **1973**, *84*, 317.
(17) Tsutsumi, K.; Shizuka, H. *Chem. Phys. Lett.* **1977**, *52*, 485.
(18) Tobita, S.; Shizuka, H. *Chem. Phys. Lett.* **1980**, *75*, 140.
(19) Shizuka, H.; Nihira, H.; Shinozaki, T. *Chem. Phys. Lett.* **1982**, *93*, 208.
(20) Shizuka, H.; Tobita, S. *J. Am. Chem. Soc*. **1982**, *104*, 6919.
(21) Shizuka, H. *Acc. Chem. Res*. **1985**, *18*, 141.
(22) Hafner, F. W. Private communication.